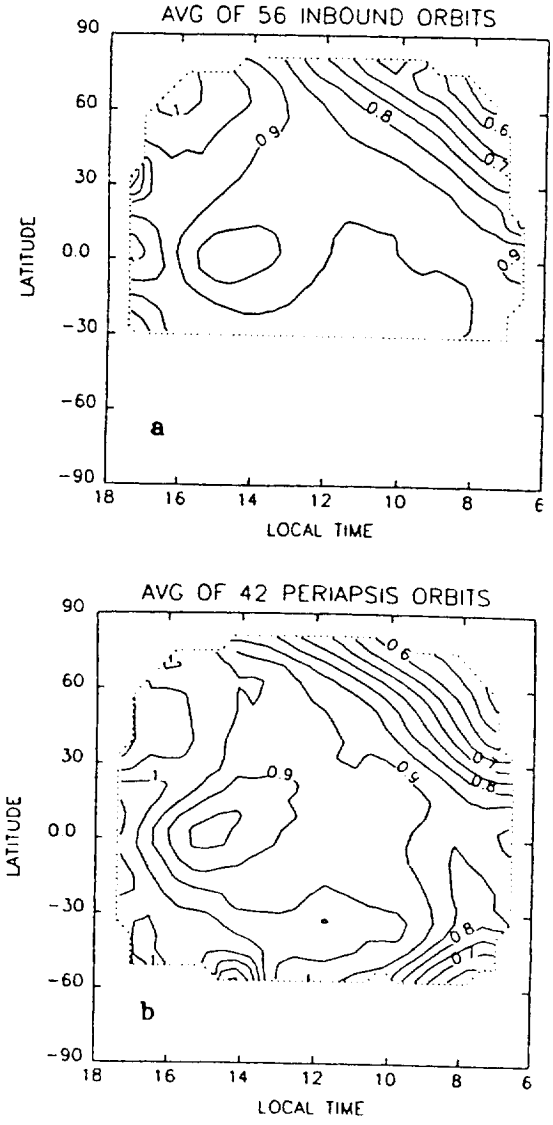

Fig. 1. Contours of brightness ratio (data/model) of the 130-nm emission displaying the local-time asymmetry (see text). The brightness ratio patterns can be thought of as anomalous patterns in O. (a) and (b) are derived from two different types of PVOUVS data: (a) contains more data, so it better displays the northern hemisphere pattern, but in (b) we can see to more southerly latitudes. The northern hemisphere pattern is mirrored there.

westward afternoon winds than with the eastward morning winds. Figure 2 shows some example eddy diffusion profiles calculated with this method. Early morning a.m. values are typically a factor of 10 or more larger than corresponding p.m. values. These local-time asymmetries will be discussed in more detail in the context of several scenarios for the middle atmosphere wave forcing. This same mechanism can also give rise to asymmetric wave drag forces that have the potential for generating the thermospheric superrotation. The mechanism for *in situ* forcing of the thermospheric superrotation is still considered a mystery, so this corollary provides strong support to our cloud-level wave source hypothesis.

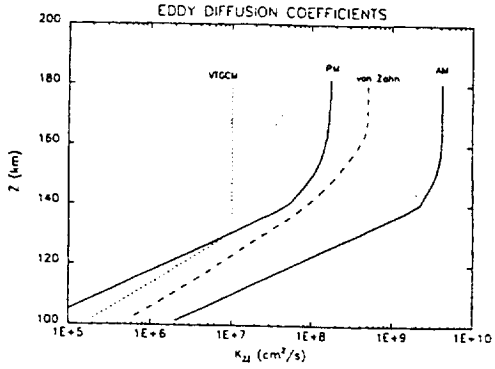

Fig. 2. Eddy diffusion coefficients characteristic of 8 a.m. and 4 p.m. wind profiles derived with the Lindzen parameterization [7]. Also shown are the VTGCM and von Zahn et al. [8] one-dimensional photochemical model K for reference.

References: [1] Bougher et al. (1988) *Icarus, 73*, 545–573. [2] Keating et al. (1986) *Adv. Space Res., 5*, 117–171. [3] Hedin et al. (1983) *JGR, 88*, 73–83. [4] Niemann et al. (1980) *JGR, 85*, 7817–7827. [5] Meier R. R. and Lee J.-S. (1982) *Planet. Space Sci., 30*, 439–450. [6] Alexander et al. (1991) *Bull. AAS, 23*, 1194. [7] Lindzen R. S. (1981) *JGR, 86*, 9707–9714. [8] von Zahn et al. (1980) *JGR, 85*, 7829–7840.

RINGED IMPACT CRATERS ON VENUS: AN ANALYSIS FROM MAGELLAN IMAGES.

Jim S. Alexopoulos and William B. McKinnon, Department of Earth and Planetary Sciences and McDonnell Center for the Space Sciences, Washington University, St. Louis MO 63130, USA.

We have analyzed cycle 1 Magellan images covering ~90% of the venusian surface and have identified 55 unequivocal peak-ring craters and multiringed impact basins. This comprehensive study (52 peak-ring craters and at least 3 multiringed impact basins) complements our earlier independent analysis of Arecibo and Venera images and initial Magellan data [1,2] and that of the Magellan team [3].

Peak-ring craters are characterized by an outer, well-defined radar-bright rim, and an inner bright ring defined by a concentric arrangement of isolated and sometimes clustered peaks. The general appearance of venusian peak-ring craters, including their inner rings and crater rims, is morphologically similar to equivalent structures on the Moon, Mars, and Mercury. Some venusian peak rings, however, are distorted in shape (noncircular outline of inner ring) and off-center. Ejecta morphologies around peak-ring craters vary from regular and symmetric, including those due to oblique impact, to irregular and asymmetric. Many peak-ring craters exhibit outflow channels. The outflows emanate from within the crater and breach the crater rim (e.g., Cleopatra), while others extend away from the distal end of the ejecta blanket or have been incorporated within the main ejecta deposit (e.g., Cochran). The interiors of most peak-ring craters are radar-dark or smooth (similar to surrounding plains), although some are bright. A few larger craters are completely flooded and show no interior structure or inner ring (e.g., Koidula, ~70 km in diameter, and Alcott, ~65 km in diameter). The radar-smooth signature of the interior is likely due to postimpact resurfacing, either volcanism or (possibly differentiated) impact

melt. Many peak-ring craters also exhibit radar-bright returns associated with rough material around peaks. Numerous central-peak structures and peak-ring craters also show darker regions at the periphery of the crater floor. These are probably areas of localized flooding, or possibly pools of impact melt. A few structures also exhibit radar-bright regions near the periphery of the floor that may represent slumped material from the crater rim. Fractures (or ridges) associated with some structures (i.e., Isabella, ~170 km in diameter, and Mona Lisa, ~81 km in diameter) exhibit a radial and concentric pattern interior to the inner ring. This tectonic fabric is the possible manifestation of stresses associated with viscous relaxation.

A plot of crater-rim to peak-ring diameter ratio against crater diameter (Fig. 1) shows that this ratio is relatively large (~5) at the transition diameter from central-peak craters and declines to less than 2 at larger diameters. The onset diameter to peak-ring forms on Venus is ~40 km [1], although peak-ring craters as small as ~30 km in diameter have now been identified (Fig. 1). The inner rings of these smaller structures are usually comprised of small, isolated, and concentrically arranged peaks, and thus are not as distinct as the coherent ring mountains of larger peak-ring craters. These smaller peak-ring forms represent transitional forms between complex craters with central and multiple peaks and well-developed peak-ring craters. The fact that ratios are larger at the transition and that ring ratios decrease with crater size is consistent with peak-ring crater formation being an extension of the process of central peak formation. Specifically, peak rings may form by hydrodynamic uplift and subsequent collapse of an increasingly unstable central peak. Upon collapse, excess material may be redistributed around the central collapse area, forming a cluster of multiple peaks or a small ring of concentrically arranged peaks. At larger scales, complete peak collapse may allow for a relatively wider redistribution of material, leading to smaller ring diameter ratios. Lending support to this argument may be the radar-bright returns associated with, and sometimes surrounding, the concentrically arranged peaks and with the central peak or peak complexes of larger complex craters. This brighter zone may be rougher material (at radar wavelength scales) associated with the central peak collapse process. On the other hand, no craters with both a peak ring and central peak have been identified, in contrast with the Moon, Mercury, and Mars. The scatter in ring ratios at a given crater diameter (Fig. 1) is real. A possible explanation is that the degree of hydrodynamic collapse of the central peak and subsequent modification, for a given crater size, depends on differences in regional postshock target rock properties (specifically, the effective viscosity and yield strength).

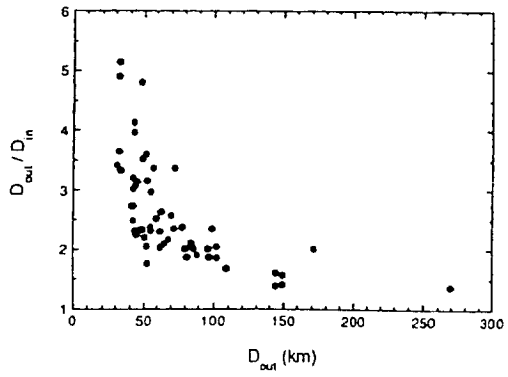

Fig. 1.

The declining ring ratio with diameter trend in Fig. 1 is similar to that observed for peak-ring craters on Mercury [1,2], albeit over a smaller-scale range. Most of the larger ringed craters with ratios of ~2 or less are similar in appearance to the smaller peak-ring forms. They exhibit an inner ring of isolated and concentrically arranged massifs (e.g., Marie Celeste, ~97 km in diameter, and Bonnevie, ~84 km in diameter), i.e., they have a distinct peak ring. However, others (e.g., Mona Lisa) exhibit very bright radar returns from continuous ridgelike portions of the inner ring that may actually be scarps. Scarplike inner rings may represent a new class of impact structure, intermediate between peak-ring craters and true multiringed basins, or the degree of floor uplift may simply be pronounced for the largest peak-ring craters. The fact that the ejecta deposits extend away from the rim of Mona Lisa means that the inner ring probably formed within the present crater rim. This is unlike venusian multiringed basins, where ejecta deposits can be seen to extend away from the first ring interior to the outer ring, implying that the outer ring formed outside what would approximate the crater rim in a smaller complex crater.

The transition from central-peak to peak-ring forms occurs at a range of diameters on the terrestrial planets that are determined mainly by surface gravity and postshock material properties [2,4]. The observed average onset diameter of ~40 km is consistent with our previous study [2] and, along with the transitions on the other terrestrial planets, supports our conclusion that the effective viscosity of cratered rubble during the modification stage is linearly proportional to crater diameter.

Of the four largest ringed craters yet identified on Venus, three appear to be multiringed impact basins. Klenova (~144 km in diameter), Lise Meitner (~148 km in diameter), and Mead (~270 km in diameter) are morphologically different from peak-ring craters, but similar to larger multiringed basin forms on the Moon, specifically Orientale. Our initial classification [1,2] of Klenova as a multiringed basin was based on the scarplike appearance of its outer rings as identified in Venera images. The Magellan image of Klenova confirms our initial interpretation. Klenova exhibits three distinct rings: an inner ring of concentrically arranged peaks (peak-ring) analogous to Orientale's Inner Rook, and two outer rings (main and intermediate) that we interpret to be possible fault scarps similar to Orientale's Cordillera ring and Outer Rook respectively. The ejecta blanket, not as evident in Venera images, is distinct and symmetrical and shows fields of secondary craters beyond the continuous ejecta deposits.

The Arecibo image of Lise Meitner exhibits two distinct radar-bright rings that we interpret to be scarplike and thus similar to Orientale's Cordillera ring and Outer Rook. The interior of Meitner is uniformly radar dark, implying a likely smooth floor of postimpact volcanic deposits. Meitner also exhibits an outer, radar-bright feature, which is at the correct spacing to be a possible partial ring, and a feature, ~9 km in width, interior to the inner ring that may be another ring or, more likely, a terrace similar to that produced by slumping of complex craters (Fig. 2). Analysis of the cycle 2 Magellan image of Meitner should better reveal the nature of these structural elements.

The largest impact structure identified on Venus, Mead, is comprised of two distinct rings. The radar-bright returns associated with each ring and an initial topographic evaluation indicate that the two rings are possible fault scarps analogous to Orientale's Cordillera ring and Outer Rook. The radar appearance of the ejecta deposits around Mead is suppressed relative to and not as distinct as that of peak-ring craters, but ejecta do occur between the two rings and extend across the outer one. The uniform radar returns associ-

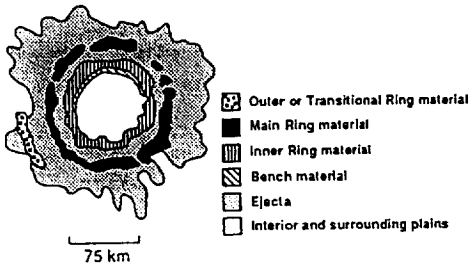

Fig. 2.

ated with Mead's interior probably indicate flooding of the topographically lower and relatively flat basin floor, with fracturing (mainly toward the center) producing locally radar-bright returns.

Isabella, with a diameter of ~170 km, is a ringed crater of the same scale, but its interior has been extensively flooded. A partially concentric arrangement of isolated peaks defines the remnants of an inner ring and a possible intermediate ring, both within the well-defined crater rim. The diameter ratio of the crater rim to the inner ring of peaks is roughly 2. If the intermediate ring, or a remnant thereof, can be shown to be scarplike in nature, then Isabella would also be a multiringed basin as interpreted here.

The ring diameter ratios of the three unequivocal multiringed impact basins are distinctly different from peak-ring craters (Fig. 1), although they follow the trend of decreasing ring ratios with increasing diameter. The ring diameter ratios for the two most distinct rings for Klenova, Meitner, and Mead are ~1.6, ~1.6, and ~1.4 respectively. Also, ring ratios for Klenova's intermediate ring to peak ring is ~1.4, as is Meitner's partial ring to main ring. These ring ratios are close to the $\sqrt{2}$ ratio suggested for Orientale and other lunar multiring basins, thus supporting the multiringed basin analogy. Finally, theoretical arguments [1,2] support the formation of multiringed basins on Venus at these scales (>100–150-km diameter).

References: [1] Alexopoulos J. S. et al. (1991) *LPSC XXII*, 13–14. [2] Alexopoulos J. S. and McKinnon W. B. (1992) *Icarus*, submitted. [3] Schaber G. G. et al. (1992) *JGR*, submitted. [4] Melosh H. J. (1989) *Impact Cratering: A Geologic Process*, Oxford, New York, 245 pp.

N93-19292

IS ISHTAR TERRA A THICKENED BASALTIC CRUST?

Jafar Arkani-Hamed, Department of Geological Sciences, McGill University, Montreal, Canada, H3A 2A7.

The mountain belts of Ishtar Terra and the surrounding tesserae are interpreted as compressional regions [1,2,3]. The gravity and surface topography of western Ishtar Terra suggest a thick crust of 60–110 km [4,5] that results from crustal thickening through tectonic processes. Underthrusting was proposed for the regions along Danu Montes [6] and Itzpapalotl Tessera [7]. Crustal thickening was suggested for the entire Ishtar Terra [8]. In this study, three lithospheric models with total thicknesses of 40, 75, and 120 km and initial crustal thicknesses of 3, 9, and 18 km are examined. These models could be produced by partial melting and chemical differentiation in the upper mantle of a colder, an Earth-like, and a hotter Venus having temperatures of respectively 1300°C, 1400°C, and 1500°C at the base of their thermal boundary layers associated with mantle convection. The effects of basalt-granulite-eclogite transformation (BGET) on the surface topography of a thickening basaltic crust is investigated adopting the experimental phase diagram [9] and density variations through the phase transformation [10].

Figure 1a shows the thermal evolution of the lithosphere of the cold Venus model with a linear crustal thickening of 0.5 km/m.y. followed by an exponential thickening for only 20 m.y. starting at 100 m.y. with a characteristic time of 20 m.y. (the main results are not very sensitive to these values; see below). Figure 1b shows the stability field of different phases that basalt enters. The BGET begins when the crust reaches a thickness of 7 km, and eclogite appears when the crust thickens beyond 70 km. Geologically speaking, the BGET is assumed to be instantaneous. Ahren and Schubert [11] suggested that cold basalt may take several tens of millions of years to transform to eclogite, and based on this suggestion Vorder Bruegge and Head [5] proposed that Maxwell Montes are 65 m.y. old. However, the recent crater distribution obtained from Magellan data suggests that the average age of Ishtar Terra is similar to that elsewhere on Venus, 500 m.y. [12,13]. To assess the effects of the time lag in the phase change, the crustal thickening is halted at 120 m.y. and the crust is allowed to reach thermal equilibrium for the next 80 m.y. The temperature increase does not significantly reduce the volume proportion of eclogite.

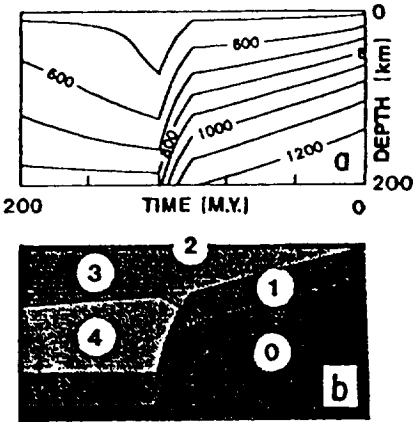

Fig. 1. Thermal evolution of the cold Venus model with a thickening crust. The numbers on the curves are temperatures in °C. Figure 1b shows the existing phases. 0 = undepleted peridotite, 1 = depleted peridotite, 2 = basaltic crust, 3 = granulite, and 4 = eclogite.

The surface topography produced by crustal thickening is determined assuming Airy isostasy with a compensation depth at 150 km as suggested for the western part of Ishtar Terra [14]. Figure 2 shows the resulting topography with (curve 1) and without (curve 2) taking into account the BGET. The density of basalt is 2900 kg/m^3 at room temperature. That of granulite increases linearly and reaches ~3500 kg/m^3 when eclogite appears. Also taken into account is the density decrease with temperature. The constant density model in Fig. 2 is similar to that of Bindschadler et al.'s [8] at steady-state condition, taking into account the density differences of the two models. However, in a more realistic model with the BGET, the surface topography attains a maximum of 1.8 km with a total crustal thickness of 38 km, beyond which the topography decreases due to sinking of the denser assemblages into the mantle. Halting the crustal thickening causes a rebound of the crust, but not enough